

Jet Luminosity of Gamma-ray Bursts: Blandford-Znajek Mechanism v.s. Neutrino Annihilation Process

Tong Liu^{1,2,3,4}, Shu-Jin Hou^{5,2}, Li Xue^{1,4}, and Wei-Min Gu^{1,4}

ABSTRACT

A neutrino-dominated accretion flow (NDAF) around a rotating stellar-mass black hole (BH) is one of the plausible candidates for the central engine of gamma-ray bursts (GRBs). Two mechanisms, i.e., Blandford-Znajek (BZ) mechanism and neutrino annihilation process, are generally considered to power GRBs. Using the analytic solutions from Xue et al. (2013) and ignoring the effects of the magnetic field configuration, we estimate the BZ and neutrino annihilation luminosities as the functions of the disk masses and BH spin parameters to contrast the observational jet luminosities of GRBs. The results show that, although the neutrino annihilation processes could account for most of GRBs, the BZ mechanism is more effective, especially for long-duration GRBs. Actually, if the energy of afterglows and flares of GRBs is included, the distinction between these two mechanisms is more significant. Furthermore, massive disk mass and high BH spin are beneficial to power high luminosities of GRBs. Finally, we discuss possible physical mechanisms to enhance the disk mass or the neutrino emission rate of NDAFs and relevant difference between these two mechanisms.

Subject headings: accretion, accretion disks - black hole physics - gamma-ray burst: general - neutrinos

¹Department of Astronomy and Institute of Theoretical Physics and Astrophysics, Xiamen University, Xiamen, Fujian 361005, China; tongliu@xmu.edu.cn

²Key Laboratory for the Structure and Evolution of Celestial Objects, Chinese Academy of Sciences, Kunming, Yunnan 650011, China

³State Key Laboratory of Theoretical Physics, Institute of Theoretical Physics, Chinese Academy of Sciences, Beijing 100190, China

⁴SHAO-XMU Joint Center for Astrophysics, Xiamen University, Xiamen, Fujian 361005, China

⁵College of Physics and Electronic Engineering, Nanyang Normal University, Nanyang, Henan 473061, China

1. Introduction

The progenitors of short-duration and long-duration gamma-ray bursts (SGRBs and LGRBs) are respectively believed to result from the merger of two compact objects, i.e., two neutron stars (NSs) or a black hole (BH) and a NS, and the core collapse of a massive star (see, e.g., Eichler et al. 1989; Paczyński 1991; Narayan et al. 1992; Woosley 1993; Paczyński 1998). A BH hyperaccretion system is expected to form in the center of gamma-ray bursts (GRBs). This geometrically thick and extremely optically thick hyperaccretion disk with high density and temperature is named the neutrino-dominated accretion flow (NDAF), which has been widely studied including the researches on the time-independent radial structure and relevant Blandford-Zanjek (BZ, Blandford & Znajek 1977) or neutrino luminosity (e.g., Popham et al. 1999; Di Matteo et al. 2002; Kohri & Mineshige 2002; Kohri et al. 2005; Gu et al. 2006; Liu et al. 2007; Kawanaka & Mineshige 2007; Lei et al. 2009; Kawanaka et al. 2013; Li & Liu 2013; Luo et al. 2013; Xue et al. 2013), on the time-independent vertical structure and relevant neutrino luminosity (e.g., Liu et al. 2008, 2010a, 2012a, 2013, 2014, 2015a), on the applications to GRBs observations (e.g., Reynoso et al. 2006; Lazzati et al. 2008; Liu et al. 2010b, 2012b; Barkov & Pozanenko 2011; Sun et al. 2012; Hou et al. 2014a,b; Liu et al. 2015b), and on the various time-dependent simulations (e.g., Ruffert & Janka 1999; Lee et al. 2004, 2009; Janiuk et al. 2013).

The magnetic field plays an important role in astrophysics, especially in high-energy astrophysics. Without exception, it is also a key role in GRBs. Two scenarios are often discussed on the central engine of GRBs. Firstly, as mentioned above, the hyperaccretion system should launch a relativistic jet to power a GRB, which origin mechanisms include neutrino-antineutrino annihilation (e.g., Popham et al. 1999; Liu et al. 2007, 2010a) and magneto-hydrodynamical process such as BZ process (e.g., Lee et al. 2000a,b; Di Matteo et al. 2002; Kawanaka et al. 2013). Secondly, apart from NDAF models, the events of the two NSs mergers or core collapses may produce a massive proto-magnetars to power GRBs and their X-ray flares (e.g., Dai et al. 2006; Metzger et al. 2011; Gao et al. 2013; Kumar & Zhang 2015; Lai 2015; Wang et al. 2015). Although the present GRBs observations cannot clearly tell us which candidate certainly exists in the center of GRBs, yet for the BH hyperaccretion process, it is still possible to contrast and identify the BZ mechanism and neutrino annihilation by the actual measurements of GRBs.

In this paper, we focus on the comparison of the jet luminosity driven by the BZ mechanism and neutrino annihilation by means of the observational data of SGRBs and LGRBs. In Section 2, we present our NDAF model and give the analytic formulae of the BZ jet power and neutrino pair annihilation. We apply these two mechanisms to explain the observation data of GRBs in order to discuss the feasibilities in Section 3. Conclusions and discussion

are in Section 4.

2. Models

In Xue et al. (2013), we investigated one-dimensional global solutions of NDAFs, taking account of general relativity in Kerr metric, neutrino physics and nucleosynthesis more precisely than most previous works (e.g, Kohri & Mineshige 2002; Kohri et al. 2005; Liu et al. 2007; Kawanaka & Mineshige 2007). In details, we considered that the total optical depth for neutrinos including scattering of electrons and nucleons and absorption through four terms, i.e., the Urca processes, electron-positron pair annihilation, nucleon-nucleon bremsstrahlung, and plasmon decay (e.g., Di Matteo et al. 2002; Liu et al. 2007). In order to allow for a transition from the optically thin to optically thick regions, a bridging formula of free protons and neutrons was established by the relations of the reaction rates in the β processes. We applied the proton-rich material in a state of nuclear statistical equilibrium (Seitenzahl et al. 2008) to NDAF model, which is suitable for almost all the range of the electron fraction. The complicated and detailed balance are included under the equilibrium of the chemical potential.

We calculated sixteen solutions with different characterized mass accretion rates and BH spins, and exhibited the radial distributions of various physical properties in NDAFs. The results showed that the gas pressure and the neutrino cooling always become dominant in the inner region for large accretion rates, and the electron degeneracy should not be ignored. Electron fraction is always about 0.46 in the outer region, and the inner, middle, and outer regions are always dominated by the free nucleons, ^4He , and ^{56}Fe .

We also calculated the neutrino luminosity and annihilation luminosity by considering the influence of neutrino trapping and proportion of heavy nuclei. Even in this case, most of the solutions show the adequate annihilation luminosities to satisfy the requirement of the mean luminosity of GRBs. Therefore, we would like to estimate the jet luminosity through the candidate BZ process or neutrino annihilation basing our results on Xue et al. (2013).

2.1. BZ Luminosity and Neutrino Annihilation Luminosity

Blandford & Znajek (1977) presented that the rotational energy of a BH can be tremendously extracted to power a Poynting jet via a large-scale poloidal magnetic field threading the horizon of the BH. The BZ luminosity can be estimated as (e.g., Krolik & Piran 2011;

Kawanaka et al. 2013)

$$L_{\text{BZ}} = f(a_*) c R_g^2 \frac{B_{\text{in}}^2}{8\pi}, \quad (1)$$

where a_* is the dimensionless BH spin, $f(a_*)$ is a factor depending on the specific configuration of the magnetic field (e.g., Blandford & Znajek 1977; Tchekhovskoy et al. 2008; Kawanaka et al. 2013), $R_g = 2GM/c^2$ is the Schwarzschild radius, M is the mass of the BH, and B_{in} is the poloidal magnetic field strength near the horizon. Moreover, the informations of the magnetic field configuration are included in $f(a_*)$. For the specified magnetic field geometries, the analytical $f(a_*)$ were attempted (e.g., Blandford & Znajek 1977; Tchekhovskoy et al. 2008), but these configurations were not required to be consistent with the dynamics of the accretion disk. Many two- or three-dimensional MHD simulations have investigated how a large-scale vertical magnetic field evolves with an accretion disk and which configurations can power a jet (e.g., McKinney & Gammie 2004; Beckwith et al. 2008, 2009; McKinney & Blandford 2009), yet the form of $f(a_*)$ is still unclear. We only know that it is an increasing function of a_* , and its range is from a small number to ~ 1 (Hawley & Krolik 2006). We consider that the structure of the magnetic field is positively important for the BZ luminosity and the structure of the disk. As simplification, we assume $f(a_*) = 1$ as well as that in Kawanaka et al. (2013), which is suitable for the fast-spinning BH in the center of GRBs.

The magnetic field energy can be estimated by the disk pressure near the horizon P_{in} presented as

$$\beta_h \frac{B_{\text{in}}^2}{8\pi} = P_{\text{in}}, \quad (2)$$

where β_h is the ratio of the midplane pressure near the horizon of the BH to the magnetic pressure in the stretched horizon. Following Kawanaka et al. (2013), we also adopt β_h to unity.

Following Xue et al. (2013), we set the BH mass $M = 3 M_\odot$ and the constant viscosity parameter $\alpha = 0.1$, which are the typical settings for GRBs. The analytic formula of the disk pressure near the horizon is a function of BH spin a_* ($0 \leq a_* < 1$) and dimensionless mass accretion rate \dot{m} ($\dot{m} \equiv \dot{M}/M_\odot \text{ s}^{-1}$, and \dot{M} is the accretion rate), which can be approximated from the data of Xue et al. (2013) as

$$\log P_{\text{in}} \text{ (erg cm}^{-3}\text{)} \approx 30.0 + 1.22a_* + 1.00 \log \dot{m}. \quad (3)$$

Under the same conditions stated above and considering the effect of the neutrino trapping, the analytic formula of the neutrino annihilation luminosity above the accretion flow

can be written as a function of BH spin and accretion rate (Xue et al. 2013)

$$\log L_{\nu\bar{\nu}} \text{ (erg s}^{-1}\text{)} \approx 49.5 + 2.45a_* + 2.17 \log \dot{m}. \quad (4)$$

We have verified that these analytic formulae are almost applicable for all the mass accretion rate higher than the ignition accretion rate.

Additionally, we noticed that the BH mass and viscosity parameter have some significant effects on the structure and components of the disk (e.g., Popham et al. 1999; Chen & Beloborodov 2007). It is noteworthy that the variation of the viscosity parameter has little effects on neutrino emission rate in the innermost region ($\lesssim 10 R_g$) of the disk. In this region, the free protons and neutrons are dominant, so the neutrino reactions related to the neutrino emission mainly occur here (e.g., Popham et al. 1999; Liu et al. 2007; Li & Liu 2013; Xue et al. 2013). In these cases with different viscosity parameters, the numbers of the launched neutrinos are roughly equal because of the similar temperatures in the innermost regions, because the cooling rate of Urca and other processes are mainly related to the temperature of the disk (e.g., Di Matteo et al. 2002). Thus the neutrino luminosity is almost independent of the viscosity value, much less the annihilation luminosity. Zalamea & Beloborodov (2011) also claimed that the uncertainty in viscosity parameter has almost no effect on annihilation luminosity. Furthermore, we calculated how the annihilation luminosity was determined by the fundamental parameters of the BH accretion system (Wang et al. 2009). It is shown that the annihilation luminosity is almost independent of α , and is not significantly related to the BH mass if it is set as several solar mass. Here only the BH spin and accretion rate are taken into account.

2.2. Methods

For SGRBs and LGRBs, if we know the isotropic luminosity L_{iso} and jet opening angle θ_{jet} or bulk Lorentz factor Γ , the jet luminosity L_{jet} can be expressed as

$$L_{\text{jet}} = L_{\text{iso}}(1 - \cos \theta_{\text{jet}}) \approx L_{\text{iso}}\Gamma^{-2}. \quad (5)$$

Moreover, the average accretion rate \dot{M} can be estimated by

$$\dot{M} \approx M_{\text{disk}}(1 + z)/T_{90}, \quad (6)$$

where M_{disk} , T_{90} , and z are the mass of the disk, the duration and redshift of GRBs, respectively. Hereafter, we would like to use the dimensionless mass of the disk defined as $m_{\text{disk}} \equiv M_{\text{disk}}/M_{\odot}$. Once the disk mass and BH spin are given, we can estimate the BZ jet

luminosity and neutrino annihilation luminosity by Equations (1) and (4). For convenience, we define two dimensionless parameter τ_1 and τ_2 as

$$\tau_1 = \log(L_{\text{jet}}/L_{\nu\bar{\nu}}), \quad (7)$$

$$\tau_2 = \log(L_{\text{jet}}/L_{\text{BZ}}), \quad (8)$$

to illustrate which mechanism is suitable for explaining SGRBs or LGRBs. It is difficult to estimate the jet opening angle independent of models, so we have to replace the angles by the calculative Lorentz factors related to the fireball model. We consider that the jet luminosity calculated from Equation (5) can also generally evaluate the BZ power.

Eichler et al. (1989) proposed that the mergers of two NSs might be the candidates for powering SGRBs. Subsequently, Ruffert & Janka (1998) reported results of three-dimensional Newtonian hydrodynamical simulations of the collision of two identical neutron stars with mass $\sim 1.6 M_{\odot}$. One of endings might be a BH $\sim 2.5 M_{\odot}$ surrounded by a disk $\sim 0.1\text{--}0.2 M_{\odot}$. The merger of a NS and a stellar-mass BH also can produce SGRBs (Paczynski 1991; Narayan et al. 1992). The simulations showed that the larger mass of the disk was formed, $\sim 0.5 M_{\odot}$ (e.g., Kluźniak & Lee 1998; Lee & Kluźniak 1999; Popham et al. 1999; Liu et al. 2012b). Woosley (1993) suggested that the core collapsar could power LGRBs, and the stellar-mass BH hyperaccretion systems might arise in the center (e.g., MacFadyen & Woosley 1999; Zhang et al. 2003), whose disk mass was about several solar mass (e.g., Popham et al. 1999). In summary, we take the typical dimensionless mass of the disk as 0.2, 0.5 and 1, 3 for SGRBs and LGRBs, respectively.

The BH spin parameter is an important ingredient for the occurrence of GRBs (e.g., Janiuk & Proga 2008; Liu et al. 2010a; Xue et al. 2013), so we choose the large spin parameters as 0.5 and 0.9 in the investigated cases, which are consistent with $f(a_*) = 1$. The detailed definition of τ for two classes of GRBs, and different typical disk masses and BH spin parameters are shown in Table 1.

3. Results

The parameters of 21 SGRBs and 55 LGRBs in our sample are presented in Tables 2 and 3, respectively, which include the redshift z , GRB duration T_{90} , isotropic mean gamma-ray luminosity L_{iso} , initial Lorentz factor Γ , and dimensionless parameters τ with different disk masses and BH spin parameters as shown in Table 1. The data are employed from Fan & Wei (2011), Lü et al. (2012), Berger (2014) and Tang et al. (2014), and the Lorentz factor of SGRBs cited from Berger (2014) are estimated by the peak time of the afterglow t_{peak} as well as methods in Fan & Wei (2011) or Lü et al. (2012). Although the calculative

Lorentz factors are related to the fireball model, we consider that the jet luminosity can also roughly evaluate the BZ power.

In these tables, the local durations of SGRBs are shorter than 2 s, conversely, durations of LGRBs are much longer than 2 s. The Lorentz factors and isotropic luminosities of LGRBs are generally larger than those of SGRBs. The parameters τ are calculated by Equations (1-8) to measure which mechanism is more effective and which set of parameters is more suitable for a certain GRB than the others as well as Figures 1 and 2.

Figures 1 and 2 display the distributions of τ for SGRBs and LGRBs under the BZ mechanism or neutrino annihilation with the different BH spins and disk masses, respectively. No matter what class or what mechanism the GRB is, the larger BH spin or larger disk mass can more effectively produce the jet luminosity of GRBs. For example, for the data of LGRBs and BZ mechanism, there are only 5 and 3 GRBs with $\tau > -3$ for the case of $m_{\text{disk}} = 1$ and $a_* = 0.5$ and the case of $m_{\text{disk}} = 3$ and $a_* = 0.5$ as the black solid lines shown in Figures 2 (a) and (b). That means the larger disk masses are more conducive to satisfy the energy requirements of GRBs. Also for the data of LGRBs and BZ mechanism, there are only 3 and 1 GRBs with $\tau > -3$ for the case of $m_{\text{disk}} = 3$ and $a_* = 0.5$ and the case of $m_{\text{disk}} = 3$ and $a_* = 0.9$ as the black solid line and dashed line shown in Figure 2 (b). That means the larger BH spin are more conducive to power GRBs. From the number distributions in the histograms, the effect of BH spin is more significant than that of disk mass for SGRBs and LGRBs.

More importantly, we should focus on the comparison between the black solid (or dashed) lines and red solid (or dashed) lines in these figures, i.e., comparison between BZ mechanisms and neutrino annihilation. Obviously, despite of the high BH spin and disk mass benefiting the high annihilation luminosity, overall the BZ power is more effective than the annihilation process for both SGRBs and LGRBs. For the SGRB cases of $m_{\text{disk}} = 0.2$ and $a_* = 0.5$, there are 3 and 0 GRBs with $\tau > 0$ respectively correspond the annihilation processes and BZ mechanism, which means that the annihilation process absolutely cannot be the candidate of the central engine in the these three SGRBs. For the SGRB cases of $m_{\text{disk}} = 0.5$ and $a_* = 0.9$, the mean τ of the BZ mechanism is also much lower than that of the annihilation process. More seriously, For LGRB cases, there are more instances cannot be explained by annihilation process.

If the neutrino annihilation process is thought to power GRBs, the jet mean power outputting is a fraction of the neutrino annihilation luminosity, and the scaling factor is considered as about 0.3 (e.g., Aloy et al. 2005; Fan & Wei 2011; Liu et al. 2015b). Actually, the more serious problem is that the energies of the afterglows and flares of GRBs are not yet included in our calculations. It is doing so in order to avoid the more dependence of model

and the uncertainty of the observational data. As we know, the energy of afterglow may be equal to or much more than that of the prompt emission, so the scaling factor may be counteracted. We ignore the efficiency problem in the radiation process that the annihilation luminosity is transferred into the jet luminosity. Thus, even $\tau < 0$ may not go far enough if the energy of afterglows and flares are about one order of magnitude higher than that of the prompt emission. As shown in figures, the distinction between two mechanisms is more significant and neutrino annihilation is more ineffective, if we consider $\tau < -1$ is reasonable.

Furthermore, the jet luminosities of GRBs 060313, 090323 and 091024 are quite higher than the other samples, so even for the BZ mechanism, higher BH spin or disk mass is required in these cases. In conclusion, the BZ mechanism is more powerful than the annihilation process. We should not only investigate which mechanism is more effective, but also find more evidences to distinguish which mechanism really exists in the center of GRBs.

4. Conclusions and Discussion

We use the analytic solutions from Xue et al. (2013) and ignore the effects of the magnetic field configuration to estimate the BZ and neutrino annihilation luminosities as the functions of the disk masses and BH spin parameters, then to contrast the observational jet luminosity of GRBs. Our results show that, although the neutrino annihilation processes could account for most of GRBs, the BZ mechanism is more effective, especially for LGRBs. Furthermore, massive disk mass and high BH spin are beneficial to power high luminosities of GRBs. Actually, there are some physical possibilities to enhance neutrino annihilation luminosity, such as increasing the disk mass or the neutrino emission rate of NDAF, and two mechanisms have possible different observational effects, which we would like to discuss below.

4.1. Disk Mass for SGRBs

The massive NSs are widely discussed in observations and theoretical models (e.g., Morrison et al. 2004; Dai et al. 2006; Li et al. 2012; Strader et al. 2015). In the past several years, the massive NSs, i.e., $\sim 2 M_{\odot}$ have been discovered by the dynamic measurements (Demorest et al. 2010; Antoniadis et al. 2013). Although their companions are white dwarfs, we cannot completely rule out the possibilities that the massive NSs exist in the binaries constituted by two NSs or a BH and a NS. Thus a massive disk $\geq 0.5 M_{\odot}$ for SGRBs may form a coalescence of a BH (or a NS) with a massive NS, i.e., $\geq 2 M_{\odot}$, and the high neutrino

annihilation luminosity could be expected. Recently, Strader et al. (2015) reported that through multiwavelength observations, a *Fermi*-LAT unidentified gamma-ray source 1FGL J1417.7-4407 may contain a massive NS (nearly $2 M_{\odot}$) and a $\sim 0.35 M_{\odot}$ giant secondary with a 5.4 day period.

Moreover, since the mergers of compact objects may produce LGRBs due to the radial transfer of the angular momentum of the massive disk (Liu et al. 2012b) and off-axis jet from collapsars may trigger SGRBs (Lazzati et al. 2010), the shortage of the accretion matter does not exhibit if some high-luminous SGRBs originate from collapsars.

Of course, we cannot neglect that the outflow from NDAFs influences the disk mass and neutrino luminosity. Janiuk et al. (2013) studied two-dimensional relativistic NDAF models and resulted that the neutrino-cooled torus launched a powerful mass outflow, which contributed to the total neutrino luminosity and mass loss from the system. We investigated the radial outflow for the angular momentum transfer, which also caused the mass loss from the disk (Liu et al. 2012b). Furthermore, for NDAFs, the high accretion rate leads to the violent evolution of the mass and spin of the central BH, which should also affect the neutrino radiation rate from the disk. In future, we will calculate the co-evolution of a BH and its surrounding NDAF to depict the more authentic pictures that indeed what happens in the center of GRBs.

4.2. Neutrino Emission Rate

Recently, Jiang et al. (2014) studied BH super-Eddington accretion flows using a global three-dimensional radiation magneto-hydrodynamical simulation. They found that the vertical advection of radiation caused by magnetic buoyancy can much effectively transport energy to increase photons emission. The similar mechanism may exist in NDAF models, which can increase neutrino emission rate. Similarly, Liu et al. (2015a) investigated the effects of the vertical convection on the structure and luminosity of the NDAF. Since the gas and neutrinos are carried to the nearby disk surface, and the convective energy transferred in the vertical direction can be effective to suppress the advection, the neutrino luminosity and annihilation luminosity are increased more than an order of magnitude for $\dot{M} \geq 1 M_{\odot} \text{ s}^{-1}$, which is conducive to achieve the energy requirement of GRBs.

Furthermore, Lei et al. (2009) and Luo et al. (2013) studied NDAF model with the magnetic coupling between the inner disk and BH. In this framework, the angular momentum and the energy can be transferred from the horizon of the BH to the disk. Thus the neutrino luminosity and relevant annihilation luminosity can be significantly enhanced to power high

luminosities of GRBs.

4.3. Polarization

If the jet powering the prompt emission and late X-ray flares of GRBs is launched by magnetic fields, GRBs are expected to be the astronomical candidate sources of linearly polarized (e.g., Fan et al. 2005). Mundell et al. (2013) reported the detection of degrees of linear polarization about 28 percent in the afterglow of LGRB GRB 120308, which might indicate that large-scale magnetic fields were presented in the GRB jets (Lai 2015). Whether high polarizations do exist in all GRB jets, future GRBs observations by the POLAR detector may further test the possibility and identify the BZ mechanism and neutrino annihilation process.

We thank the anonymous referee for very useful suggestions and comments. This work was supported by the National Basic Research Program of China (973 Program) under grant 2014CB845800, the National Natural Science Foundation of China under grants 11222328, 11233006, 11333004, 11373002, 11473022, and U1331101, the CAS Open Research Program of Key Laboratory for the Structure and Evolution of Celestial Objects under grants OP201305 and OP201403.

REFERENCES

- Aloy, M. A., Janka, H.-T., & Müller, E. 2005, *A&A*, 436, 273
- Antoniadis, J., Freire, P. C. C., Wex, N., et al. 2013, *Science*, 340, 448
- Barkov, M. V., & Pozanenko, A. S. 2011, *MNRAS*, 417, 2161
- Beckwith, K., Hawley, J. F., & Krolik, J. H. 2008, *ApJ*, 678, 1180
- Beckwith, K., Hawley, J. F., & Krolik, J. H. 2009, *ApJ*, 707, 428
- Berger, E. 2014, *ARA&A*, 52, 43
- Blandford, R. D., & Znajek, R. L. 1977, *MNRAS*, 179, 433
- Chen, W. X., & Beloborodov, A. M. 2007, *ApJ*, 657, 383
- Dai, Z. G., Wang, X. Y., Wu, X. F., & Zhang, B. 2006, *Science*, 311, 1127
- Demorest, P. B., Pennucci, T., Ransom, S. M., Roberts, M. S. E., & Hessels, J. W. T. 2010, *Nature*, 467, 1081
- Di Matteo, T., Perna, R., & Narayan, R. 2002, *ApJ*, 579, 706
- Eichler, D., Livio, M., Piran, T., & Schramm, D. N. 1989, *Nature*, 340, 126
- Fan Y. Z., Zhang B., Proga D., 2005, *ApJL*, 635, L129
- Fan, Y.-Z., & Wei, D.-M. 2011, *ApJ*, 739, 47
- Gao, H., Ding, X., Wu, X.-F., Zhang, B., & Dai, Z.-G. 2013, *ApJ*, 771, 86
- Gu, W.-M., Liu, T., & Lu, J.-F. 2006, *ApJ*, 643, L87
- Hawley, J. F., & Krolik, J. H. 2006, *ApJ*, 641, 103
- Hou, S.-J., Gao, H., Liu, T., et al. 2014a, *MNRAS*, 441, 2375
- Hou, S.-J., Liu, T., Gu, W.-M., et al. 2014b, *ApJ*, 781, L19
- Janiuk, A., Mioduszewski, P., & Moscibrodzka, M. 2013, *ApJ*, 776, 105
- Janiuk, A., & Proga, D. 2008, *ApJ*, 675, 519
- Jiang, Y.-F., Stone, J. M., & Davis, S. W. 2014, *ApJ*, 796, 106

- Kawanaka, N., & Mineshige, S. 2007, *ApJ*, 662, 1156
- Kawanaka, N., Piran, T., & Krolik, J. H. 2013, *ApJ*, 766, 31
- Kluźniak, W., & Lee, W. H. 1998, *ApJ*, 494, L53
- Kohri, K., & Mineshige, S. 2002, *ApJ*, 577, 311
- Kohri, K., Narayan, R., & Piran, T. 2005, *ApJ*, 629, 341
- Krolik, J. H., & Piran, T. 2011, *ApJ*, 743, 134
- Kumar, P., & Zhang, B. 2015, *Phys. Rep.*, 561, 1
- Lai, D. 2015, *Space Sci. Rev.*, 14
- Lazzati, D., Morsony, B. J., & Begelman, M. C. 2010, *ApJ*, 717, 239
- Lazzati, D., Perna, R., & Begelman, M. C. 2008, *MNRAS*, 388, L15
- Lee, H. K., Brown, G. E., & Wijers, R. A. M. J. 2000a, *ApJ*, 536, 416
- Lee, H. K., Wijers, R. A. M. J., & Brown, G. E. 2000b, *Phys. Rep.*, 325, 83
- Lee, W. H., & Kluźniak, W. 1999, *ApJ*, 526, 178
- Lee, W. H., Ramirez-Ruiz, E., & Page, D. 2004, *ApJ*, 608, L5
- Lee, W. H., Ramirez-Ruiz, E., & López-Cámara, D. 2009, *ApJ*, 699, L93
- Lei, W. H., Wang, D. X., Zhang, L., et al. 2009, *ApJ*, 700, 1970
- Li, A., Huang, F., & Xu, R.-X. 2012, *Astroparticle Physics*, 37, 70
- Li, A., & Liu, T. 2013, *A&A*, 555, A129
- Liu, T., Gu, W.-M., Dai, Z.-G., & Lu, J.-F. 2010a, *ApJ*, 709, 851
- Liu, T., Gu, W.-M., Kawanaka, N., & Li, A. 2015a, *ApJ*, in press, arXiv:1503.04054
- Liu, T., Gu, W.-M., Xue, L., & Lu, J.-F. 2007, *ApJ*, 661, 1025
- Liu, T., Gu, W.-M., Xue, L., Weng, S.-S., & Lu, J.-F. 2008, *ApJ*, 676, 545
- Liu, T., Gu, W.-M., Xue, L., & Lu, J.-F. 2012a, *Ap&SS*, 337, 711
- Liu, T., Liang, E.-W., Gu, W.-M., et al. 2010b, *A&A*, 516, A16

- Liu, T., Liang, E.-W., Gu, W.-M., et al. 2012b, *ApJ*, 760, 63
- Liu, T., Lin, Y.-Q., Hou, S.-J., & Gu, W.-M. 2015b, *ApJ*, in press, arXiv:1504.02156
- Liu, T., Xue, L., Gu, W.-M., & Lu, J.-F. 2013, *ApJ*, 762, 102
- Liu, T., Yu, X.-F., Gu, W.-M., & Lu, J.-F. 2014, *ApJ*, 791, 69
- Luo, Y., Gu, W.-M., Liu, T., & Lu, J.-F. 2013, *ApJ*, 773, 142
- Lü, J., Zou, Y.-C., Lei, W.-H., et al. 2012, *ApJ*, 751, 49
- MacFadyen, A. I., & Woosley, S. E. 1999, *ApJ*, 524, 262
- McKinney, J. C., & Blandford, R. D. 2009, *MNRAS*, 394, L126
- McKinney, J. C., & Gammie, C. F. 2004, *ApJ*, 611, 977
- Metzger, B. D., Giannios, D., Thompson, T. A., Bucciantini, N., & Quataert, E. 2011, *MNRAS*, 413, 2031
- Morrison, I. A., Baumgarte, T. W., & Shapiro, S. L. 2004, *ApJ*, 610, 941
- Mundell, C. G., Kopač, D., Arnold, D. M., et al. 2013, *Nature*, 504, 119
- Narayan, R., Paczyński, B., & Piran, T. 1992, *ApJ*, 395, L83
- Paczynski, B. 1991, *Acta Astronomica*, 41, 257
- Paczynski, B. 1998, *ApJ*, 494, L45
- Popham, R., Woosley, S. E., & Fryer, C. 1999, *ApJ*, 518, 356
- Reynoso, M. M., Romero, G. E., & Sampayo, O. A. 2006, *A&A*, 454, 11
- Ruffert, M., & Janka, H.-T. 1998, *A&A*, 338, 535
- Ruffert, M., & Janka, H.-T. 1999, *A&A*, 344, 573
- Seitenzahl, I. R., Timmes, F. X., Marin-Lafèche, A., et al. 2008, *ApJ*, 685, L129
- Strader, J., Chomiuk, L., Cheung, C. C., et al. 2015, *ApJ*, in press, arXiv:1502.05999
- Sun, M.-Y., Liu, T., Gu, W.-M., & Lu, J.-F. 2012, *ApJ*, 752, 31
- Tang, Q.-W., Peng, F.-K., Wang, X.-Y., & Tam, P.-H. T. 2014, arXiv:1412.3342

- Tchekhovskoy, A., McKinney, J. C., & Narayan, R. 2008, MNRAS, 388, 551
- Wang, H., Liu, T., & Lu, J.-F. 2009, Science in China: Physics, Mechanics and Astronomy, 52, 729
- Wang, L.-J., Dai, Z.-G., & Yu, Y.-W. 2015, ApJ, 800, 79
- Woosley, S. E. 1993, ApJ, 405, 273
- Xue, L., Liu, T., Gu, W.-M., & Lu, J.-F. 2013, ApJS, 207, 23
- Zalamea, I., & Beloborodov, A. M. 2011, MNRAS, 410, 2302
- Zhang, W., Woosley, S. E., & MacFadyen, A. I. 2003, ApJ, 586, 356

Table 1: Definition of τ

	τ_{11}^S	τ_{12}^S	τ_{21}^S	τ_{22}^S	τ_{13}^S	τ_{14}^S	τ_{23}^S	τ_{24}^S
Class ¹	S	S	S	S	S	S	S	S
Mechanism ²	1	1	2	2	1	1	2	2
a_*	0.5	0.5	0.5	0.5	0.9	0.9	0.9	0.9
m_{disk}	0.2	0.5	0.2	0.5	0.2	0.5	0.2	0.5
	τ_{11}^L	τ_{12}^L	τ_{21}^L	τ_{22}^L	τ_{13}^L	τ_{14}^L	τ_{23}^L	τ_{24}^L
Class	L	L	L	L	L	L	L	L
Mechanism	1	1	2	2	1	1	2	2
a_*	0.5	0.5	0.5	0.5	0.9	0.9	0.9	0.9
m_{disk}	1	3	1	3	1	3	1	3

¹Class: S - SGRBs; L - LGRBs.

²Mechanism: 1 - neutrino annihilation process; 2 - BZ mechanism.

Table 2. Data of SGRBs

SGRB	z	T_{90} (s)	$L_{\text{iso}}(10^{52} \text{ erg s}^{-1})$	Γ	Ref. ¹	τ_{11}^S	τ_{12}^S	τ_{21}^S	τ_{22}^S	τ_{13}^S	τ_{14}^S	τ_{23}^S	τ_{24}^S
021211	1.006	2.3	0.98	195	a	-1.67	-2.53	-4.24	-4.64	-2.65	-3.51	-4.73	-5.13
040924	0.858	2.39	1.17	490	a	-2.28	-3.15	-4.92	-5.31	-3.26	-4.13	-5.40	-5.80
050709	0.16	0.07	0.11	4.76	b	-2.15	-3.02	-3.23	-3.63	-3.13	-4.00	-3.71	-4.11
050724	0.257	3	0.02	5	b	0.44	-0.43	-2.51	-2.91	-0.54	-1.41	-3.00	-3.39
051210	1.3	1.3	0.63	39.34	c	-1.14	-2.00	-3.35	-3.75	-2.12	-2.98	-3.84	-4.24
051221A	0.55	1.4	0.27	10	b	0.12	-0.74	-2.33	-2.73	-0.86	-1.72	-2.82	-3.22
060313	1.7	0.7	31.09	7.05	c	1.32	0.45	-0.50	-0.90	0.34	-0.53	-0.99	-1.39
061006	0.4377	0.4	0.75	9.09	b	-0.45	-1.32	-2.31	-2.70	-1.43	-2.30	-2.79	-3.19
061201	0.11	0.8	0.01	3.52	c	-0.50	-1.37	-2.84	-3.24	-1.48	-2.35	-3.33	-3.73
070714B	0.92	3	0.08	12.5	b	-0.10	-0.96	-2.83	-3.23	-1.08	-1.94	-3.31	-3.71
070724A	0.46	0.4	0.06	3.5	c	-0.76	-1.62	-2.60	-3.00	-1.74	-2.60	-3.09	-3.49
070809	0.47	1.3	0.06	8.04	c	-0.33	-1.20	-2.78	-3.17	-1.31	-2.18	-3.26	-3.66
071112c	0.82	0.3	0.51	6	c	-0.75	-1.62	-2.34	-2.74	-1.73	-2.60	-2.83	-3.22
071227	0.381	1.8	0.04	11.11	b	-0.40	-1.27	-3.04	-3.44	-1.38	-2.25	-3.53	-3.92
080905A	0.12	1	0.01	11.18	c	-1.69	-2.55	-4.13	-4.53	-2.67	-3.53	-4.62	-5.02
090426	2.609	1.25	0.87	16.67	b	-0.71	-1.58	-2.68	-3.08	-1.69	-2.56	-3.17	-3.56
090510	0.903	0.3	40.3	123	b	-1.52	-2.39	-3.09	-3.49	-2.50	-3.37	-3.57	-3.97
090515	0.4	0.04	0.30	30.99	c	-4.07	-4.94	-4.77	-5.16	-5.05	-5.92	-5.25	-5.65
100117A	0.92	0.3	1.30	37.23	c	-1.98	-2.85	-3.54	-3.94	-2.96	-3.83	-4.03	-4.43
100625A	0.45	0.3	0.57	19.07	c	-1.50	-2.36	-3.20	-3.60	-2.48	-3.34	-3.69	-4.08
100816A	0.8035	2.8	0.37	100	b	-1.22	-2.08	-3.95	-4.35	-2.20	-3.06	-4.44	-4.83

¹References: (a) Lü et al. (2012); (b) Fan & Wei (2011); (c) Berger (2014).

Table 3. Data of LGRBs

LGRB	z	$T_{90}(\text{s})$	$L_{\text{iso}}(10^{52} \text{ erg s}^{-1})$	Γ	Ref. ¹	τ_{11}^L	τ_{12}^L	τ_{21}^L	τ_{22}^L	τ_{13}^L	τ_{14}^L	τ_{23}^L	τ_{24}^L
990123	1.61	63.3	9.44	600	a	-0.30	-1.34	-3.61	-4.09	-1.28	-2.32	-4.10	-4.57
050401	2.9	33	4.14	590	a	-1.64	-2.67	-4.41	-4.89	-2.62	-3.65	-4.90	-5.37
050525A	0.606	8.8	1.74	229	a	-1.60	-2.64	-4.15	-4.63	-2.58	-3.62	-4.64	-5.12
050730	3.97	155	0.29	201	a	-0.63	-1.66	-4.06	-4.54	-1.61	-2.64	-4.55	-5.03
050801	1.56	20	0.12	420	a	-2.95	-3.99	-5.69	-6.16	-3.93	-4.97	-6.17	-6.65
050820A	2.615	600	0.58	282	a	0.96	-0.08	-3.33	-3.81	-0.02	-1.06	-3.82	-4.29
050922C	2.198	4.54	3.56	274	a	-2.72	-3.75	-4.58	-5.06	-3.70	-4.73	-5.07	-5.55
060210	3.91	220	0.93	264	a	-0.02	-1.05	-3.64	-4.11	-1.00	-2.03	-4.12	-4.60
060418	1.49	52	0.48	263	a	-1.02	-2.06	-4.25	-4.73	-2.00	-3.04	-4.74	-5.21
060605	3.8	19	0.63	197	a	-2.22	-3.25	-4.60	-5.08	-3.20	-4.23	-5.09	-5.57
060607A	3.082	100	0.37	296	a	-1.08	-2.12	-4.40	-4.87	-2.06	-3.10	-4.88	-5.36
060904B	0.703	192	0.01	108	a	-0.53	-1.57	-4.62	-5.10	-1.51	-2.55	-5.11	-5.58
060908	2.43	19.3	1.90	304	a	-1.78	-2.82	-4.35	-4.83	-2.76	-3.80	-4.83	-5.31
061007	1.262	75	3.16	436	a	-0.20	-1.24	-3.67	-4.15	-1.18	-2.22	-4.16	-4.63
061121	1.314	81	0.75	175	a	0.01	-1.02	-3.48	-3.96	-0.97	-2.00	-3.97	-4.44
070110	2.352	89	0.21	127	a	-0.52	-1.56	-3.87	-4.35	-1.50	-2.54	-4.36	-4.84
070318	0.84	63	0.04	143	a	-1.08	-2.12	-4.57	-5.04	-2.06	-3.10	-5.05	-5.53
070411	2.954	101	0.39	208	a	-0.72	-1.75	-4.05	-4.53	-1.70	-2.73	-4.54	-5.01
070419A	0.97	112	0.0042	91	a	-1.21	-2.25	-4.95	-5.43	-2.19	-3.23	-5.44	-5.92
071003	1.1	148	0.97	283	a	0.37	-0.67	-3.48	-3.96	-0.61	-1.65	-3.97	-4.44
071010A	0.98	6	0.04	101	a	-3.06	-4.09	-5.31	-5.78	-4.04	-5.07	-5.79	-6.27
071010B	0.947	35.74	0.14	209	a	-1.48	-2.51	-4.64	-5.12	-2.46	-3.49	-5.13	-5.61
071031	2.692	150.49	0.10	133	a	-0.50	-1.53	-4.07	-4.54	-1.48	-2.51	-4.55	-5.03
080129	4.394	48	0.79	65	a	-0.39	-1.43	-3.19	-3.67	-1.37	-2.41	-3.68	-4.15
080319B	0.937	57	4.49	580	a	-0.41	-1.45	-3.82	-4.30	-1.39	-2.43	-4.30	-4.78
080319C	1.95	29.55	2.25	228	a	-0.92	-1.95	-3.78	-4.25	-1.90	-2.93	-4.26	-4.74
080330	1.51	61	0.02	104	a	-1.52	-2.56	-4.83	-5.31	-2.50	-3.54	-5.32	-5.79
080413B	1.1	8.0	0.47	128	a	-2.01	-3.04	-4.37	-4.85	-2.99	-4.02	-4.86	-5.34
080603A	1.688	150	0.03	88	a	-0.39	-1.43	-4.12	-4.60	-1.37	-2.41	-4.61	-5.09
080710	0.845	120	0.01	63	a	-0.31	-1.35	-4.12	-4.60	-1.29	-2.33	-4.61	-5.08
080810	3.35	108	1.21	409	a	-0.84	-1.87	-4.16	-4.64	-1.82	-2.85	-4.64	-5.12
080916C	4.35	66	71.33	1130	a	-0.61	-1.65	-3.57	-4.05	-1.59	-2.63	-4.06	-4.54
081203A	2.1	223	0.24	219	a	0.004	-1.03	-3.86	-4.33	-0.98	-2.01	-4.34	-4.82
090313	3.375	78	0.18	136	a	-1.02	-2.06	-4.17	-4.65	-2.00	-3.04	-4.66	-5.14
090323	3.568	150	12.15	110	a	1.57	0.53	-1.89	-2.37	0.59	-0.45	-2.38	-2.86
090328A	0.736	70	0.57	540	a	-0.95	-1.99	-4.52	-4.99	-1.93	-2.97	-5.00	-5.48
090424	0.544	49.47	0.12	300	a	-1.33	-2.37	-4.78	-5.26	-2.31	-3.35	-5.27	-5.74
090812	2.452	75.09	1.85	501	a	-0.96	-1.99	-4.21	-4.68	-1.94	-2.97	-4.69	-5.17
090902B	1.8229	21.9	41.25	120	a	0.66	-0.37	-2.07	-2.54	-0.32	-1.35	-2.55	-3.03
090926A	2.1062	20	29.35	150	a	0.15	-0.89	-2.49	-2.96	-0.83	-1.87	-2.97	-3.45
091024	1.092	1020	0.06	69	a	2.19	1.15	-2.65	-3.12	1.21	0.17	-3.13	-3.61
091029	2.752	39.18	0.71	221	a	-1.35	-2.39	-4.23	-4.71	-2.33	-3.37	-4.72	-5.19
100621A	0.542	63.6	0.11	52	a	0.39	-0.65	-3.19	-3.66	-0.59	-1.63	-3.67	-4.15
100724B	1.00	111.6	0.98	162	b	0.64	-0.40	-3.09	-3.57	-0.34	-1.38	-3.58	-4.06
100728B	2.106	12.1	0.77	373	a	-2.70	-3.74	-5.08	-5.55	-3.68	-4.72	-5.56	-6.04
100906A	1.727	114.4	0.80	369	a	-0.43	-1.47	-4.02	-4.50	-1.41	-2.45	-4.51	-4.98

Table 3—Continued

LGRB	z	$T_{90}(\text{s})$	$L_{\text{iso}}(10^{52} \text{ erg s}^{-1})$	Γ	Ref. ¹	τ_{11}^L	τ_{12}^L	τ_{21}^L	τ_{22}^L	τ_{13}^L	τ_{14}^L	τ_{23}^L	τ_{24}^L
110205A	2.22	257	0.70	177	a	0.75	-0.28	-3.16	-3.64	-0.23	-1.26	-3.65	-4.12
110213A	1.46	48	0.33	223	a	-1.10	-2.14	-4.30	-4.78	-2.08	-3.12	-4.79	-5.26
130504C	1.00	74	0.58	144	b	0.12	-0.91	-3.40	-3.87	-0.86	-1.89	-3.88	-4.36
130518	2.49	48	10.0	257	b	-0.07	-1.11	-3.09	-3.57	-1.05	-2.09	-3.58	-4.06
130821A	1.00	84	0.69	72	b	0.92	-0.11	-2.67	-3.14	-0.06	-1.09	-3.15	-3.63
131108A	2.40	19	8.52	907	b	-2.09	-3.12	-4.65	-5.13	-3.07	-4.10	-5.14	-5.61
131231A	0.642	31	0.54	192	b	-0.79	-1.83	-3.97	-4.45	-1.77	-2.81	-4.46	-4.93
140206B	1.00	120	1.28	254	b	0.43	-0.60	-3.34	-3.81	-0.55	-1.58	-3.82	-4.30
141028A	2.332	31.5	6.11	397	b	-1.02	-2.05	-3.85	-4.32	-2.00	-3.03	-4.33	-4.81

¹References: (a) Lü et al. (2012); (b) Tang et al. (2014).

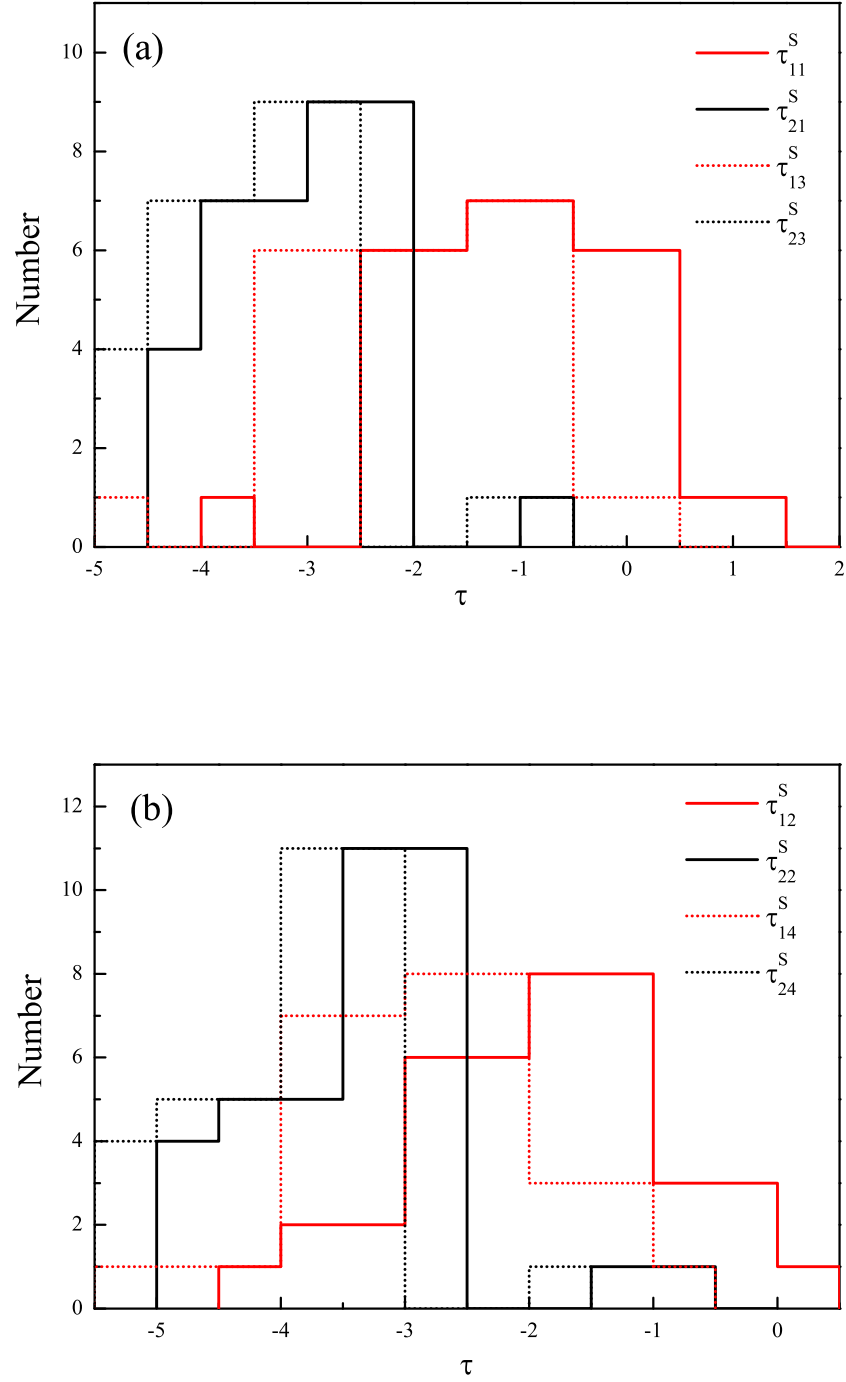


Fig. 1.— Distributions of τ for SGRBs under the BZ mechanism or neutrino annihilation with the different BH spins and disk masses.

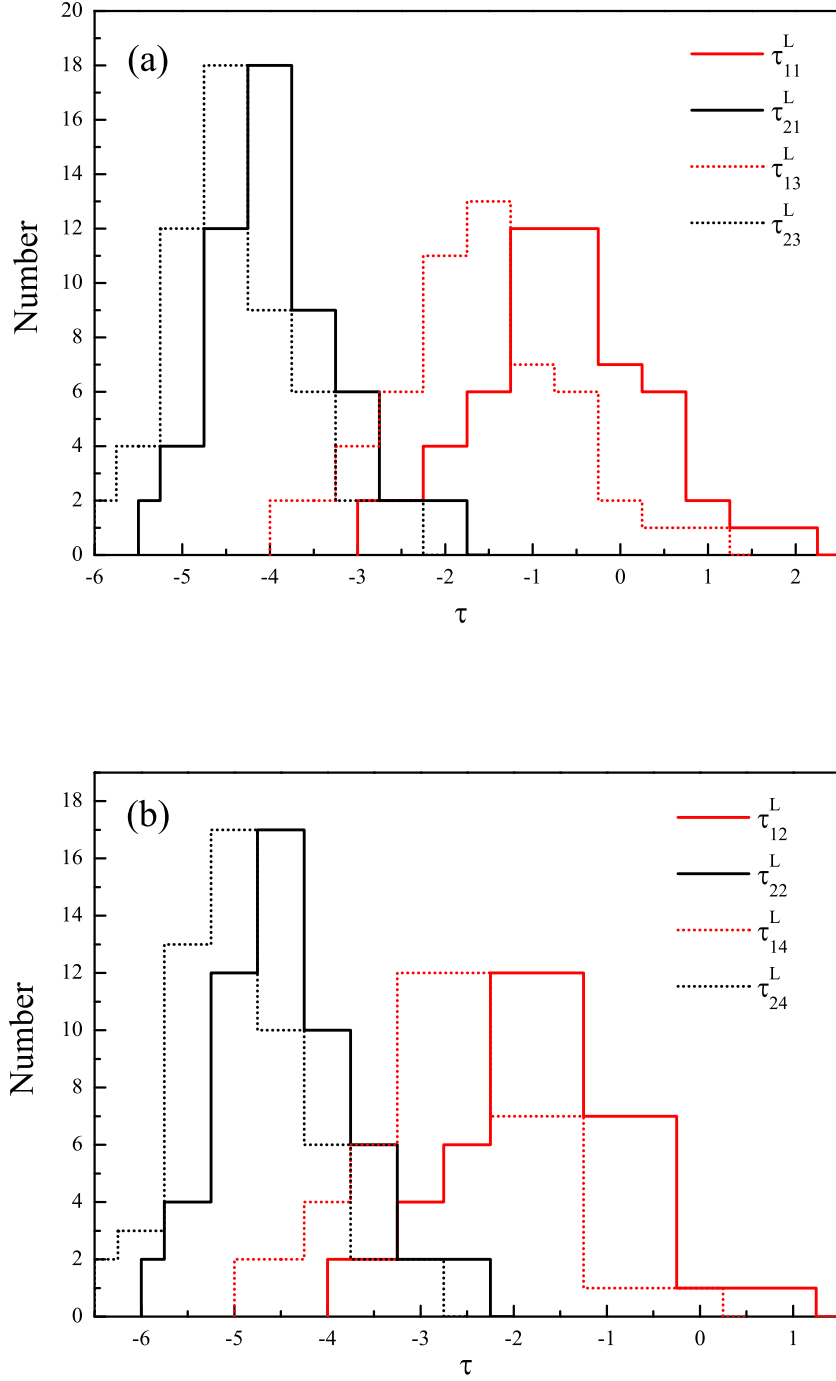


Fig. 2.— Distributions of τ for LGRBs under the BZ mechanism or neutrino annihilation with the different BH spins and disk masses.